Time-dependent transport through single molecules: nonequilibrium Greens functions and TDDFT ⋆

1 Introduction

The nomenclature *quantum transport* has been coined for the phenomenon of electron motion through constrictions of transverse dimensions smaller than the electron wavelength, *e.g.*, quantum-point contacts, quantum wires, molecules, etc. To describe transport properties on such a small scale, a quantum theory of transport is required. In this section we focus on quantum transport problems whose experimental setup is schematically displayed in Fig. 1a. A central region of meso- or nano-scopic size is coupled to two metallic electrodes which play the role of charge reservoirs. The whole system is initially in a well defined equilibrium configuration, described by a *unique* temperature and chemical potential (thermodynamic consistency). No current flows through the junction, the charge density of the electrodes being perfectly balanced. As originally proposed by Cini [1], we may drive the system out of equilibrium by exposing the electrons to an external time-dependent potential which is local in time and space. For instance, we may switch on an electric field by putting the system between two capacitor plates far away from the system boundaries, see Fig. 1b. The dynamical formation of dipole layers screens the potential-drop along the electrodes and the total potential turns out to be uniform in the left and right bulks. Accordingly, the potential-drop is entirely limited to the central region. As the system size increases the remote parts are less disturbed by the junction and the density inside the electrodes approaches the equilibrium bulk-density.

There has been considerable activity to describe transport through these systems on an *ab initio* level. Most approaches are based on a self-consistency procedure first proposed by Lang [2]. In this steady-state approach based on density functional theory (DFT), exchange and correlation is approximated by the static local-density potential and the charge density is obtained self-consistently in the presence of the steady current. However, the original justification involved subtle points such as different Fermi levels deep inside the left and right electrodes and the implicit reference of non-local perturbations such as tunneling Hamiltonians within a DFT framework. (For a

⋆ Contributed by Gianluca Stefanucci, Carl-Olof Almbladh, Stefan Kurth, E. K. U. Gross, Angel Rubio, Robert van Leeuwen, Nils Erik Dahlen and Ulf von Barth

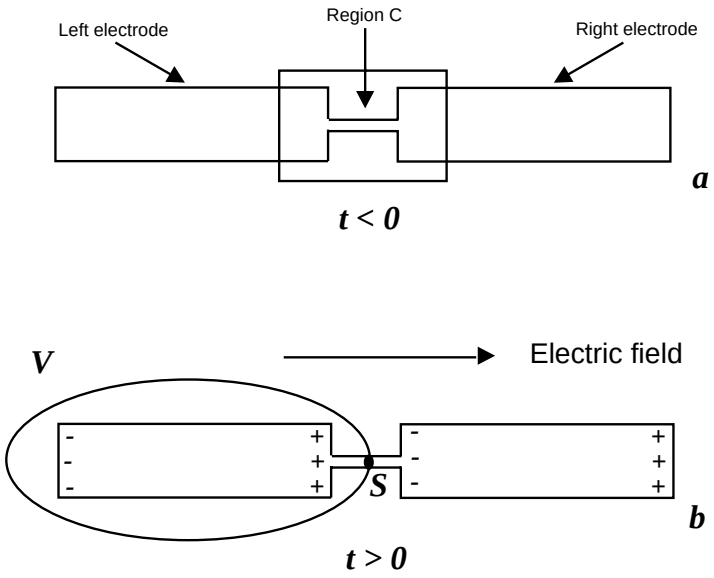

Fig. 1. Schematic sketch of the experimental setup described in the main text. A central region which also includes few layers of the left and right electrodes is coupled to macroscopically large metallic reservoirs. a) The system is in equilibrium for negative times. b) At positive times the electrons experience an electric field generated by two capacitor plates far away from the system boundaries. Discarding retardation effects, the screening of the potential-drop in the electrodes is instantaneous and the total potential turns out to be uniform in the left and right electrodes separately.

detailed discussion we refer to Ref. [3].) The steady-state DFT approach has been further developed [4–7] and the results have been most useful for understanding the qualitative behavior of measured current-voltage characteristics. Quantitatively, however, the theoretical I-V curves typically differ from the experimental ones by several orders of magnitude [8]. Several explanations are possible for such a mismatch: models are not sufficiently refined, parasitic effects in measurements have been underestimated, the characteristics of the molecule-contact interfaces are not well understood and difficult to address given their atomistic complexity. Another theoretical reason for this discrepancy might be the fact that the transmission functions computed from static DFT have resonances at the non-interacting Kohn-Sham excitation energies which in general do not coincide with the true excitation energies. Further-

more, different exchange-correlation functionals lead to DFT-currents that vary by more than an order of magnitude [9].

On the other hand, excitation energies of interacting systems are accessible via time-dependent (TD) DFT [10,11]. In this theory, the time-dependent density of an interacting system moving in an external, time-dependent local potential can be calculated via a fictitious system of non-interacting electrons moving in a local, effective time-dependent potential. Therefore this theory is in principle well suited for the treatment of nonequilibrium transport problems [3,12]. Below, we combine the Cini scheme with TDDFT and we describe in detail how TDDFT can be used to calculate the time-dependent current in systems like the one of Fig. 1. The theoretical formulation of an exact theory based on TDDFT and nonequilibrium Green functions (NEG) has been developed in Ref. [3] and shortly after used for conductance calculations of molecular wires [13]. A practical scheme to go beyond static calculations and perform the full time evolution has recently been proposed by Kurth *et al.* [14]. The theory was originally developed for systems initially described by a thermal density matrix. An extension to unbalanced (out of equilibrium) initial states can be found in Ref. [15].

Here we also mention that another thermodynamically consistent scheme has been proposed by Kamenev and Kohn [16]. They consider a closed system (ring) and drive it out of equilibrium by switching an external vector potential. As the Cini scheme, this approach also overcomes the problem of having two or more chemical potentials. Since the Kamenev-Kohn approach uses a vector potential rather than a scalar potential, TD current DFT (TDCDFT) would be the natural density-functional extension.

2 An exact formulation based on TDDFT

In quantum transport problems like the one discussed in the previous Section, we are mainly interested in calculating the total current through the junction rather than the current density in some point of the system. Assuming that the electrons can leave the region of volume V in Fig. 1b only through the surface S, then the total time-dependent current $I_S(t)$ is given by the time derivative of the total number of particles in volume V. Denoting by $n(\mathbf{r},t)$ the particle density we have

$$I_S(t) = -e \int_V \mathrm{d}\mathbf{r} \frac{\mathrm{d}}{\mathrm{d}t} n(\mathbf{r},t). \tag{1}$$

Runge and Gross have shown that $n(\mathbf{r},t)$ can be computed in a one-particle manner provided it falls off rapidly enough for $\mathbf{r} \to \infty$ (this theory applies only to those cases where the external disturbance is local in space). Therefore, we may calculate $n(\mathbf{r},t)$, and in turn $I_S(t)$, by solving a fictitious non-interacting problem described by an effective Hamiltonian $\boldsymbol{H}_s(t)$. The potential $v_s(\mathbf{r},t)$ experienced by the electrons in $\boldsymbol{H}_s(t)$ is called the

Kohn-Sham (KS) potential and it is given by the sum of the external potential, the Coulomb potential of the nuclei, the Hartree potential and the exchange-correlation potential $v_{\rm xc}$. The latter accounts for the complicated many-body effects and is obtained from an exchange-correlation action functional, $v_{\rm xc}(\mathbf{r},t)=\delta A_{\rm xc}[n]/\delta n(\mathbf{r},t)$ (as pointed out in Ref. [17], the causality and symmetry properties require that the action functional $A_{\rm xc}[n]$ is defined on the Keldysh contour). $A_{\rm xc}$ is a functional of the density and of the initial density matrix. In our case, the initial density matrix is the thermal density matrix which, due to the extension of the Hohenberg-Kohn theorem [18] to finite temperatures [19], also is a functional of the density.

Without loss of generality we will assume that the external potential vanishes for times $t\leq 0$. The initial equilibrium density is then given by $\sum_s f(e_s)|\langle\mathbf{r}|\psi_s(0)\rangle|^2$, where f is the Fermi function. The KS states $|\psi_s(0)\rangle$ are eigenstates of $\boldsymbol{H}_s(0)$ with KS energies e_s. For positive times, the time-dependent density can be calculated by evolving the KS states according to the Schrödinger equation

$$\mathrm{i}\frac{\mathrm{d}}{\mathrm{d}t}|\psi_s(t)\rangle=\boldsymbol{H}_s(t)|\psi_s(t)\rangle. \tag{2}$$

Thus,

$$n(\mathbf{r},t)=\sum_s f(e_s)\,|\langle\mathbf{r}|\psi_s(t)\rangle|^2, \tag{3}$$

and the continuity equation, $\dot{n}(\mathbf{r},t)=-\boldsymbol{\nabla}\cdot\mathbf{j}_{\rm KS}(\mathbf{r},t)$, can be written in terms of the KS current density

$$\mathbf{j}_{\rm KS}(\mathbf{r},t)=-\sum_s f(e_s)\,{\rm Im}[\psi_s^*(\mathbf{r},t)\boldsymbol{\nabla}\psi_s(\mathbf{r},t)], \tag{4}$$

where $\psi_s(\mathbf{r},t)=\langle\mathbf{r}|\psi_s(t)\rangle$ are the time-dependent KS orbitals. Using Gauss theorem and the continuity equation it is straightforward to obtain

$$I_S(t)=e\sum_s f(e_s)\int_S \mathrm{d}\sigma\;\hat{\mathbf{n}}\cdot{\rm Im}[\psi_s^*(\mathbf{r},t)\boldsymbol{\nabla}\psi_s(\mathbf{r},t)], \tag{5}$$

where $\hat{\mathbf{n}}$ is the unit vector perpendicular to the surface element $\mathrm{d}\sigma$.

The switching on of an electric field excites plasmon oscillations which dynamically screen the external disturbance. Such a metallic screening prevents any rearrangements of the initial equilibrium bulk-density, provided the time-dependent perturbation is slowly varying during a typical plasmon time-scale (which is usually less than a fs). Thus, the KS potential v_s undergoes a uniform time-dependent shift deep inside the left and right electrodes and the KS potential-drop is entirely limited to the central region.

Let us now consider an electric field constant in time. After the transient phase, the current will slowly decrease. We expect a very long plateau with superimposed oscillations, whose amplitude is inversely proportional to the

system size. As the size of the electrodes increases the amplitude of the oscillations decreases and the plateau phase become successively longer. The steady-state current is defined as the current at the plateau for infinitely large electrodes.

What is the physical mechanism leading to a steady-state current? In the real system, dissipative effects like electron-electron or electron-phonon scatterings provide a natural explanation for the damping of the transient oscillations and the onset of a steady state. However, in the fictitious KS system the electrons are non-interacting and the damping mechanisms of the real problem are described by the local potential $v_{\rm xc}$. We conclude that for any non-interacting system having the geometry of Fig. 1, there must be a class of time-dependent local potentials leading to a steady current. Below, we use the NEG techniques to study under what circumstances a steady-state current develops and what is the underlying physical mechanism. We also show that the steady-current can be expressed in a Landauer-like formula in terms of fictitious transmission coefficients and one-particle energy eigenvalues.

3 Non-equilibrium Green functions

The one-particle scheme of TDDFT corresponds to a fictitious Green function $\boldsymbol{\mathcal{G}}(z;z')$ which satisfies a one-particle equation of motion on the Keldysh contour of Fig. 2,

$$\left\{\mathrm{i}\frac{\mathrm{d}}{\mathrm{d}z}-\boldsymbol{H}_s(z)\right\}\boldsymbol{\mathcal{G}}(z;z')=\delta(z;z'). \tag{6}$$

It is convenient to define the projectors $P_\alpha=\int_\alpha d\mathbf{r}|\mathbf{r}\rangle\langle\mathbf{r}|$ onto the left or right electrodes ($\alpha=L,R$) or the central region ($\alpha=C$). Although the $\mathbf{r}$ basis is not differentiable, the diagonal and off-diagonal matrix elements of the kinetic energy remain well defined in a distribution sense. We introduce the notation

$$\boldsymbol{\mathcal{O}}_{\alpha\beta}\equiv P_\alpha\boldsymbol{\mathcal{O}}P_\beta, \tag{7}$$

where $\boldsymbol{\mathcal{O}}$ is an arbitrary operator in one-body space. Here and in what follows, we use boldface for operators in one-particle Hilbert space. The uncontacted KS Hamiltonian is $\boldsymbol{\mathcal{E}}\equiv\boldsymbol{H}_{s_{LL}}+\boldsymbol{H}_{s_{CC}}+\boldsymbol{H}_{s_{RR}}$ while $\boldsymbol{V}\equiv\boldsymbol{H}_s-\boldsymbol{\mathcal{E}}$ accounts for the contacting part. Since $\boldsymbol{V}_{LR}=\boldsymbol{V}_{RL}=0$, from Eqs. (1-6) the current from the $\alpha=L,R$ electrode to the central region is

$$\begin{aligned}I_\alpha(t)&=e\int\mathrm{d}\mathbf{r}\;\mathrm{i}\frac{\mathrm{d}}{\mathrm{d}t}\langle\mathbf{r}|\boldsymbol{\mathcal{G}}^<_{\alpha\alpha}(t;t)|\mathbf{r}\rangle\\&=e\int\mathrm{d}\mathbf{r}\,\langle\mathbf{r}|\boldsymbol{V}_{\alpha C}\boldsymbol{\mathcal{G}}^<_{C\alpha}(t;t)-\boldsymbol{\mathcal{G}}^<_{\alpha C}(t;t)\boldsymbol{V}_{C\alpha}|\mathbf{r}\rangle.\end{aligned} \tag{8}$$

We define the one-particle operator $\boldsymbol{Q}_\alpha(t)$ in the central subregion C as

$$\boldsymbol{Q}_\alpha(t)=\boldsymbol{\mathcal{G}}^<_{C\alpha}(t;t)\boldsymbol{V}_{\alpha C} \tag{9}$$

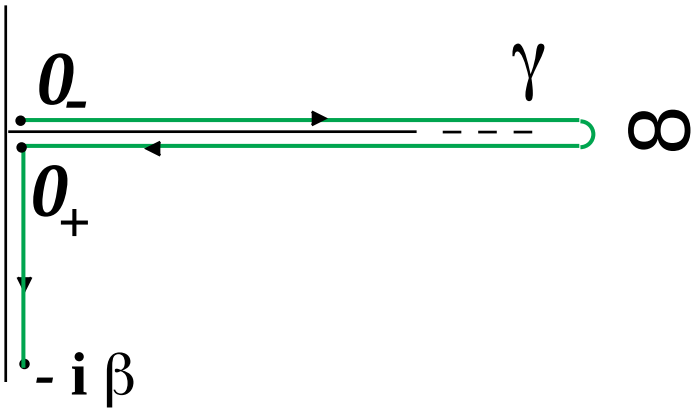

Fig. 2. The Keldysh contour γ is an oriented contour with endpoints in 0_- and $-\mathrm{i}\beta$, β being the inverse temperature. It constitutes of a forward branch going from 0_- to ∞, a backward branch coming back from ∞ to 0_+ and a vertical (thermic) track on the imaginary time axis between 0_+ and $-\mathrm{i}\beta$. The variables z and z' run on γ.

and write the total current in Eq. (8) as

$$I_\alpha(t) = 2e\,\mathrm{Re}\left[\mathrm{Tr}\,\{\boldsymbol{Q}_\alpha(t)\}\right], \quad \alpha = L, R, \tag{10}$$

where the symbol Tr denotes the trace over a complete set of one-particle states of C.

For the noninteracting system of TDDFT everything is known once we know how to propagate the one-electron orbitals in time and how they are populated before the system is perturbed. The time evolution is fully described by the retarded or advanced Green functions $\boldsymbol{\mathcal{G}}^{\mathrm{R,A}}$, and the initial population at zero time, *i.e.*, by $\boldsymbol{\mathcal{G}}^{<}(0,0) = if(\boldsymbol{H}_s(0))$, where f is the Fermi distribution function [since $\boldsymbol{H}_s(0)$ is a matrix, so is $f(\boldsymbol{H}_s(0))$]. Then, for any $t, t' > 0$ we have [1,12,20]

$$\boldsymbol{\mathcal{G}}^{<}(t,t') = i\,\boldsymbol{\mathcal{G}}^{\mathrm{R}}(t,0) f(\boldsymbol{H}_s(0)) \boldsymbol{\mathcal{G}}^{\mathrm{A}}(0,t') = \boldsymbol{\mathcal{G}}^{\mathrm{R}}(t,0)\boldsymbol{\mathcal{G}}^{<}(0,0)\boldsymbol{\mathcal{G}}^{\mathrm{A}}(0,t'), \tag{11}$$

and hence

$$\boldsymbol{Q}_\alpha(t) = \Big[\boldsymbol{\mathcal{G}}^{\mathrm{R}}(t,0)\boldsymbol{\mathcal{G}}^{<}(0,0)\boldsymbol{\mathcal{G}}^{\mathrm{A}}(0,t)\Big]_{C\alpha}\,\boldsymbol{V}_{\alpha C}. \tag{12}$$

The above equation is an *exact* result. For noninteracting electrons, Eq. (12) agrees with the formula obtained by Cini [1]. Indeed, the derivation by Cini does not depend on the details of the noninteracting system and therefore it is also correct for the Kohn-Sham system, which however has the extra merit of reproducing the exact density. The advantage of this approach is that the interaction in the leads and in the conductor are treated on the same footing

via self-consistent calculations on the current-carrying system. It also allows for detailed studies of how the contacts influence the conductance properties. We note in passing that Eq. (12) is also gauge invariant since it does not change under an overall time-dependent shift of the external potential which is constant in space. It is also not modified by a simultaneous shift of the classical electrostatic potential and the chemical potential for $t < 0$.

Let us now focus on the long-time behavior and work out a simplified expression. We introduce the uncontacted Green function $\boldsymbol{g}$ which obeys Eq. (6) with $\boldsymbol{V} = 0$,

$$\left\{ \mathrm{i}\frac{\mathrm{d}}{\mathrm{d}z} - \boldsymbol{\mathcal{E}}(z) \right\} \boldsymbol{g}(z;z') = \delta(z;z'). \tag{13}$$

The $\boldsymbol{g}$ can be expressed in terms of the one-body evolution operator $\boldsymbol{\mathcal{S}}(t)$ which fullfils

$$\mathrm{i}\frac{\mathrm{d}}{\mathrm{d}t}\boldsymbol{\mathcal{S}}(t) = \boldsymbol{\mathcal{E}}(t)\boldsymbol{\mathcal{S}}(t), \qquad \text{with} \quad \boldsymbol{\mathcal{S}}(0) = \mathbf{1}. \tag{14}$$

The retarded and advanced components are

$$\boldsymbol{g}^{\mathrm{R,A}}(t;t') = \mp i\,\Theta(\pm t \mp t')\boldsymbol{\mathcal{S}}(t)\boldsymbol{\mathcal{S}}^{\dagger}(t'), \tag{15}$$

while the lesser component $\boldsymbol{g}^{<}(t;t') = i\boldsymbol{g}^{\mathrm{R}}(t;0)f(\boldsymbol{\mathcal{E}}(0))\boldsymbol{g}^{\mathrm{A}}(0;t)$, since also the uncontacted system is initially in equilibrium [cf. Eq (11)].

We convert the equation of motion for $\boldsymbol{\mathcal{G}}$ into an integral equation

$$\boldsymbol{\mathcal{G}}(z;z') = \boldsymbol{g}(z;z') + \int_{\gamma} \mathrm{d}\bar{z}\, \boldsymbol{g}(z;\bar{z})\boldsymbol{V}\boldsymbol{\mathcal{G}}(\bar{z};z'), \tag{16}$$

γ being the Keldysh contour of Fig. 2. The TDDFT Green function $\boldsymbol{\mathcal{G}}$ projected in a subregion $\alpha = L, R$ or C can be described in terms of self-energies which account for the hopping in and out of the subregion in question. Considering the central region, the self-energy can be written as

$$\boldsymbol{\Sigma}(z;z') = \sum_{\alpha=L,R} \boldsymbol{\Sigma}_{\alpha}, \quad \boldsymbol{\Sigma}_{\alpha}(z;z') = \boldsymbol{V}_{C\alpha}\,\boldsymbol{g}(z;z')\boldsymbol{V}_{\alpha C}. \tag{17}$$

Eqs. (16-17) allow to express $\boldsymbol{Q}_{\alpha}$ in terms of the projected Green function onto the central region, $\boldsymbol{G} \equiv \boldsymbol{\mathcal{G}}_{CC}$, and $\boldsymbol{\Sigma}$. Below we shall make an extensive use of the Keldysh book-keeping of Section 2.2. After some tedious algebra one finds

$$\begin{aligned}
\boldsymbol{Q}_{\alpha}(t) = & \sum_{\beta=L,R} \left[\boldsymbol{G}^{\mathrm{R}} \cdot \boldsymbol{\Sigma}^{<}_{\beta} \cdot \left(\delta_{\beta\alpha} + \boldsymbol{G}^{\mathrm{A}} \cdot \boldsymbol{\Sigma}^{\mathrm{A}}_{\alpha} \right) \right](t;t) \\
& + \sum_{\beta=L,R} \left[\boldsymbol{G}^{\mathrm{R}} \cdot \boldsymbol{\Sigma}^{\rceil} \star \boldsymbol{G}^{\mathrm{M}} \star \boldsymbol{\Sigma}^{\lceil}_{\beta} \cdot \left(\delta_{\beta\alpha} + \boldsymbol{G}^{\mathrm{A}} \cdot \boldsymbol{\Sigma}^{\mathrm{A}}_{\alpha} \right) \right](t;t) \\
& + i \sum_{\beta=L,R} \boldsymbol{G}^{\mathrm{R}}(t;0) \left[\boldsymbol{G}^{\mathrm{M}} \star \boldsymbol{\Sigma}^{\lceil}_{\beta} \cdot \left(\delta_{\beta\alpha} + \boldsymbol{G}^{\mathrm{A}} \cdot \boldsymbol{\Sigma}^{\mathrm{A}}_{\alpha} \right) \right](0;t) \\
& + \left(\boldsymbol{G}^{\mathrm{R}}(t;0)\boldsymbol{G}^{\mathrm{M}}(0;0) - i \left[\boldsymbol{G}^{\mathrm{R}} \cdot \boldsymbol{\Sigma}^{\rceil} \star \boldsymbol{G}^{\mathrm{M}} \right](t;0) \right) \left[\boldsymbol{G}^{\mathrm{A}} \cdot \boldsymbol{\Sigma}^{\mathrm{A}}_{\alpha} \right](0;t).
\end{aligned} \tag{18}$$

Here we briefly explain the notation used. The symbol "$\cdot$" is used to write $\int_0^\infty \mathrm{d}\bar{t} f(\bar{t})g(\bar{t})$ as $f\cdot g$, while the symbol "$\star$" is used to write $\int_0^{-\mathrm{i}\beta} \mathrm{d}\bar{\tau} f(\bar{\tau})g(\bar{\tau})$ as $f\star g$. The superscripts "M", "$\rceil$", "$\lceil$" in Green functions or self-energies denote the Matsubara component (both arguments on the thermic imaginary track), the Keldysh component with a real first argument and an imaginary second argument and the Keldysh component with an imaginary first argument and a real second argument, respectively.

Let us now take both the left and right electrodes infinitely large and thereafter consider the limit of $t \to \infty$. Then, only the first term on the r.h.s. of Eq. (18) does not vanish as both $\boldsymbol{G}$ and $\boldsymbol{\Sigma}$ tend to zero when the separation between their time argument increases. Thus, the long-time limit washes out the initial effect induced by the conducting term $\boldsymbol{V}$. Moreover, the asymptotic current is independent of the initial equilibrium distribution of the central device. We expect that for small bias the electrons at the bottom of the left and right conducting bands are not disturbed and the transient process is exponentially short. On the other hand, for strong bias the transient phase might decay as a power law, due to possible band-edge singularities.

Using the asymptotic $(t, t' \to \infty)$ relation [12]

$$\boldsymbol{G}^<(t;t') = \left[\boldsymbol{G}^\mathrm{R}\cdot\boldsymbol{\Sigma}^<\cdot\boldsymbol{G}^\mathrm{A}\right](t;t') \tag{19}$$

we may write the asymptotic time-dependent current as

$$I_\alpha(t) = 2e\,\mathrm{Re}\left[\mathrm{Tr}\left\{\left[\boldsymbol{G}^\mathrm{R}\cdot\boldsymbol{\Sigma}^<_\alpha\right](t;t) + \left[\boldsymbol{G}^<\cdot\boldsymbol{\Sigma}^\mathrm{A}_\alpha\right](t;t)\right\}\right]. \tag{20}$$

Eq. (20) is valid for interacting devices connected to interacting electrodes, since the non-interacting TDDFT Green function gives the exact density. It also provides a useful framework for studying the transport in interacting systems from first principles. It can be applied both to the case of a constant (d.c.) bias as well as to the case of a *time-dependent* (*e.g.*, a.c.) one. For noninteracting electrons the Green function $\boldsymbol{\mathcal{G}}$ of TDDFT coincides with the Green function of the real system and Eq. (20) agrees with the formula by Wingreen *et al.* [21,22].

4 Steady state

Let us now consider an external potential having a well defined limit when $t \to \infty$. Taking first the thermodynamic limit of the two electrodes and afterward the limit $t \to \infty$ we expect that the KS Hamiltonian $\boldsymbol{H}_s(t)$ will *globally* converge to an asymptotic KS Hamiltonian $\boldsymbol{H}_s^\infty$, meaning that $\lim_{t\to\infty}\boldsymbol{\mathcal{E}}(t) = \boldsymbol{\mathcal{E}}^\infty = \text{const}$. In this case it must exist a unitary operator $\bar{\boldsymbol{\mathcal{S}}}$ such that

$$\lim_{t\to\infty}\boldsymbol{\mathcal{S}}(t) = \exp[-\mathrm{i}\boldsymbol{\mathcal{E}}^\infty t]\,\bar{\boldsymbol{\mathcal{S}}}. \tag{21}$$

Then, in terms of diagonalising one-body states $|\psi^{\infty}_{m\alpha}\rangle$ of $\boldsymbol{\mathcal{E}}^{\infty}_{\alpha\alpha}$ with eigenvalues $e^{\infty}_{m\alpha}$ we have

$$\boldsymbol{\Sigma}^{<}_{\alpha}(t;t') = \mathrm{i}\sum_{m,m'} \mathrm{e}^{-\mathrm{i}[e^{\infty}_{m\alpha}t - e^{\infty}_{m'\alpha}t']}\boldsymbol{V}_{C\alpha}|\psi^{\infty}_{m\alpha}\rangle\langle\psi^{\infty}_{m\alpha}|f(\bar{\boldsymbol{\mathcal{E}}}^{0})|\psi^{\infty}_{m'\alpha}\rangle\langle\psi^{\infty}_{m'\alpha}|\boldsymbol{V}_{\alpha C}, \tag{22}$$

where $\bar{\boldsymbol{\mathcal{E}}}^{0} = \bar{\boldsymbol{\mathcal{S}}}\ \boldsymbol{\mathcal{E}}^{0}\bar{\boldsymbol{\mathcal{S}}}^{\dagger}$ and $\boldsymbol{\mathcal{E}}^{0} \equiv \boldsymbol{\mathcal{E}}(t=0)$. For $t, t' \to \infty$, the left and right contraction with a nonsingular $\boldsymbol{V}$ causes a perfect destructive interference for states with $|e^{\infty}_{m\alpha} - e^{\infty}_{m'\alpha}| \gtrsim 1/(t+t')$ and hence the restoration of translational invariance in time

$$\boldsymbol{\Sigma}^{<}_{\alpha}(t;t') = \mathrm{i}\sum_{m} f_{m\alpha}\boldsymbol{\Gamma}_{m\alpha}\mathrm{e}^{-\mathrm{i}e^{\infty}_{m\alpha}(t-t')}, \tag{23}$$

where $f_{m\alpha} = \langle\psi^{\infty}_{m\alpha}|f(\bar{\boldsymbol{\mathcal{E}}}^{0})|\psi^{\infty}_{m\alpha}\rangle$ while $\boldsymbol{\Gamma}_{m\alpha} = \boldsymbol{V}_{C\alpha}|\psi^{\infty}_{m\alpha}\rangle\langle\psi^{\infty}_{m\alpha}|\boldsymbol{V}_{\alpha C}$ [23]. The above *dephasing mechanism* is the key ingredient for the appearance of a steady state. Substituting Eq. (23) into Eq. (20) we get the steady state current

$$I_{\alpha} = -2e\sum_{m\beta} f_{m\beta}\Big[\mathrm{Tr}\left\{\boldsymbol{G}^{\mathrm{R}}(e^{\infty}_{m\beta})\boldsymbol{\Gamma}_{m\beta}\boldsymbol{G}^{\mathrm{A}}(e^{\infty}_{m\beta})\mathrm{Im}[\boldsymbol{\Sigma}^{\mathrm{A}}_{\alpha}(e^{\infty}_{m\beta})]\right\} + \delta_{\beta\alpha}\mathrm{Tr}\left\{\boldsymbol{\Gamma}_{m\alpha}\mathrm{Im}[\boldsymbol{G}^{\mathrm{R}}(e^{\infty}_{m\alpha})]\right\}\Big] \tag{24}$$

with $\boldsymbol{G}^{\mathrm{R,A}}(\varepsilon) = [\varepsilon - \boldsymbol{\mathcal{E}}^{\infty}_{CC} - \boldsymbol{\Sigma}^{\mathrm{R,A}}(\varepsilon)]^{-1}$. Using the equalities

$$\mathrm{Im}[\boldsymbol{G}^{\mathrm{R}}] = \frac{1}{2\mathrm{i}}[\boldsymbol{G}^{\mathrm{R}} - \boldsymbol{G}^{\mathrm{A}}], \qquad [\boldsymbol{G}^{\mathrm{R}} - \boldsymbol{G}^{\mathrm{A}}] = [\boldsymbol{G}^{>} - \boldsymbol{G}^{<}] \tag{25}$$

together with

$$[\boldsymbol{G}^{>}(\varepsilon) - \boldsymbol{G}^{<}(\varepsilon)] = -2\pi\mathrm{i}\sum_{m\alpha}\delta(\varepsilon - e^{\infty}_{m\alpha})\boldsymbol{G}^{\mathrm{R}}(e^{\infty}_{m\alpha})\boldsymbol{\Gamma}_{m\alpha}\boldsymbol{G}^{\mathrm{A}}(e^{\infty}_{m\alpha}) \tag{26}$$

and

$$\mathrm{Im}[\boldsymbol{\Sigma}^{\mathrm{A}}_{\alpha}(\varepsilon)] = \pi\sum_{m}\delta(\varepsilon - e^{\infty}_{m\alpha})\boldsymbol{\Gamma}_{m\alpha}, \tag{27}$$

the steady-state current in Eq. (24) can be rewritten in a Landauer-like [24] form

$$J_R = -e\sum_{m}[f_{mL}\mathcal{T}_{mL} - f_{mR}\mathcal{T}_{mR}] = -J_L. \tag{28}$$

In the above formula $\mathcal{T}_{mR} = \sum_n \mathcal{T}^{nL}_{mR}$ and $\mathcal{T}_{mL} = \sum_n \mathcal{T}^{nR}_{mL}$ are the TDDFT transmission coefficients expressed in terms of the quantities

$$\mathcal{T}^{n\beta}_{m\alpha} = 2\pi\delta(e^{\infty}_{m\alpha} - e^{\infty}_{n\beta})\mathrm{Tr}\left\{\boldsymbol{G}^{\mathrm{R}}(e^{\infty}_{m\alpha})\boldsymbol{\Gamma}_{m\alpha}\boldsymbol{G}^{\mathrm{A}}(e^{\infty}_{n\beta})\boldsymbol{\Gamma}_{n\beta}\right\} = \mathcal{T}^{m\alpha}_{n\beta}. \tag{29}$$

Despite the formal analogy with the Landauer formula, Eq. (28) contains an important conceptual difference since $f_{m\alpha}$ is not simply given by the Fermi

distribution function. For example, if the induced change in effective potential varies widely in space deep inside the electrodes, the band structure $\bar{\boldsymbol{\mathcal{E}}}^0_{\alpha\alpha}$ may be completely different from that of $\boldsymbol{\mathcal{E}}^\infty_{\alpha\alpha}$. However, if we asymptotically have equilibrium far away from the central region, as we would expect for electrodes with a macroscopic cross section, the change in effective potential must be uniform. To leading order in $1/N$ we then have

$$\boldsymbol{\mathcal{E}}_{\alpha\alpha}(t) = \boldsymbol{\mathcal{E}}^0_{\alpha\alpha} + \delta v_\alpha(t), \tag{30}$$

and $\boldsymbol{\mathcal{E}}^\infty_{\alpha\alpha} = \boldsymbol{\mathcal{E}}^0_{\alpha\alpha} + \delta v_{\alpha,\infty}$. Hence, except for corrections which are of lower order with respect to the system size, $\bar{\boldsymbol{\mathcal{E}}}^0_{\alpha\alpha} = \boldsymbol{\mathcal{E}}^0_{\alpha\alpha}$ and

$$f_{m\alpha} = f(e^\infty_{m\alpha} - \delta v_{\alpha,\infty}). \tag{31}$$

We emphasize that the steady-state current in Eq. (28) results from a pure dephasing mechanism in the fictitious noninteracting problem. The damping effects of scattering are described by $A_{\rm xc}$ and $v_{\rm xc}$. Furthermore, the current depends only on the asymptotic value of the KS potential, $v_s(\mathbf{r}, t \to \infty)$, provided that Eq. (30) holds. However, $v_s(\mathbf{r}, t \to \infty)$ might depend on the history of the external applied potential and the resulting steady-state current might be history dependent. In these cases the full time evolution can not be avoided. In the case of Time Dependent Local Density Approximation (TDLDA), the exchange-correlation potential $v_{\rm xc}$ depends only locally on the instantaneous density and has no memory at all. If the density tends to a constant, so does the KS potential v_s, which again implies that the density tends to a constant. Owing to the non-linearity of the problem there might still be more than one steady-state solution or none at all.

5 A practical implementation scheme

The total time-dependent current $I_S(t)$ can be calculated from the KS orbitals according to Eq. (5). However, before a TDDFT calculation of transport can be tackled, a number of technical problems have to be addressed. In particular, one needs a practical scheme for extracting the set of initial states of the infinitely large system and for propagating them. Of course, since one can in practice only deal with finite systems this can only be achieved by applying the correct boundary conditions. The problem of so-called "transparent boundary conditions" for the time-dependent Schrödinger equation has been attacked by many authors. For a recent overview, the reader is referred to Ref. [25]. Below, we sketch how to compute the initial extended states and how to propagate them (we refer to Ref. [14] for the explicit implementation of the algorithm).

The KS eigenstate $\psi_{s=Ej}$ of the Hamiltonian $\boldsymbol{H}_s(0)$ is uniquely specified by its eigenenergy E and a label j for the degenerate orbitals of this energy.

It is possible to show that the eigenfunctions of $\mathrm{Im}[\boldsymbol{\mathcal{G}}^{\mathrm{R}}_{CC}(E)]$ can be expressed as a linear combination of the ψ_{Ej} projected onto the central region. If we use N_g grid points to describe the central region, the diagonalization in principle gives N_g eigenvectors but only a few have the physical meaning of extended eigenstates at this energy. It is, however, very easy to identify the physical states by looking at the eigenvalues: only few eigenvalues are nonvanishing. The corresponding states are the physical ones. All the other eigenvalues are zero (or numerically close to zero) and the corresponding states have no physical meaning. This procedure gives the correct extended eigenstates in the central region only up to a normalization factor. When diagonalizing $\mathrm{Im}[\boldsymbol{\mathcal{G}}^{\mathrm{R}}_{CC}(E)]$ with typical library routines one obtains eigenvectors which are normalized to the central region. Physically this might be incorrect. Therefore, the normalization has to be fixed separately. This can be done by matching the wavefunction for the central region to the known form (and normalization) of the wavefunction in the macroscopic leads.

Once the initial states have been calculated we need a suitable algorithm for propagating them. The explicitly treated region C includes the first few atomic layers of the left and right electrodes. The boundaries of this region are chosen in such a way that the density outside C is accurately described by an equilibrium bulk density. It is convenient to write $\boldsymbol{\mathcal{E}}_{\alpha\alpha}(t)$, with $\alpha = L, R$, as the sum of a term $\boldsymbol{\mathcal{E}}_{\alpha}$ which is constant in time and another term $\boldsymbol{U}_{\alpha}(t)$ which is explicitly time-dependent, $\boldsymbol{\mathcal{E}}_{\alpha\alpha}(t) = \boldsymbol{\mathcal{E}}_{\alpha} + \boldsymbol{U}_{\alpha}(t)$. In configuration space $\boldsymbol{U}_{\alpha}(t)$ is diagonal at any time t since the KS potential is local in space. Furthermore, the diagonal elements $U_{\alpha}(\mathbf{r}, t)$ are spatially constant for metallic electrodes. Thus, $\boldsymbol{U}_{\alpha}(t) = U_{\alpha}(t)\mathbf{1}_{\alpha}$ and $U_L(t) - U_R(t)$ is the total potential drop across the central region. Here $\mathbf{1}_{\alpha}$ is the unit operator for region α. We write $\boldsymbol{H}_s(t) = \boldsymbol{\mathcal{E}}(t) + \boldsymbol{V} = \tilde{\boldsymbol{H}}(t) + \boldsymbol{U}(t)$, with $\boldsymbol{U}(t) = \boldsymbol{U}_L(t) + \boldsymbol{U}_R(t)$. For any given initial state $\psi(0) = \psi^{(0)}$ we calculate $\psi(t_m = m\Delta t) = \psi^{(m)}$ by using a generalized form of the Cayley method

$$(\mathbf{1} + \mathrm{i}\delta\tilde{\boldsymbol{H}}^{(m)})\frac{\mathbf{1} + \mathrm{i}\frac{\delta}{2}\boldsymbol{U}^{(m)}}{\mathbf{1} - \mathrm{i}\frac{\delta}{2}\boldsymbol{U}^{(m)}}\psi^{(m+1)} = (\mathbf{1} - \mathrm{i}\delta\tilde{\boldsymbol{H}}^{(m)})\frac{\mathbf{1} - \mathrm{i}\frac{\delta}{2}\boldsymbol{U}^{(m)}}{\mathbf{1} + \mathrm{i}\frac{\delta}{2}\boldsymbol{U}^{(m)}}\psi^{(m)}, \quad (32)$$

with $\tilde{\boldsymbol{H}}^{(m)} = \frac{1}{2}[\tilde{\boldsymbol{H}}(t_{m+1}) + \tilde{\boldsymbol{H}}(t_m)]$, $\boldsymbol{U}^{(m)} = \frac{1}{2}[\boldsymbol{U}(t_{m+1}) + \boldsymbol{U}(t_m)]$ and $\delta = \Delta t/2$. It should be noted that our propagator is norm conserving (unitary) and accurate to second-order in δ, as is the Cayley propagator. Denoting by ψ_{α} the projected wave function onto the region $\alpha = R, L, C$, we find from Eq. (32)

$$\psi_C^{(m+1)} = \frac{\mathbf{1} - \mathrm{i}\delta\boldsymbol{H}^{(m)}_{\mathrm{eff}}}{\mathbf{1} + \mathrm{i}\delta\boldsymbol{H}^{(m)}_{\mathrm{eff}}}\psi_C^{(m)} + S^{(m)} - M^{(m)}. \quad (33)$$

Here, $\boldsymbol{H}^{(m)}_{\mathrm{eff}}$ is the effective Hamiltonian of the central region:

$$\boldsymbol{H}^{(m)}_{\mathrm{eff}} = \boldsymbol{\mathcal{E}}^{(m)}_{CC} - \boldsymbol{V}_{CL}\frac{\mathrm{i}\delta}{\mathbf{1} + \mathrm{i}\delta\boldsymbol{\mathcal{E}}_L}\boldsymbol{V}_{LC} - \boldsymbol{V}_{CR}\frac{\mathrm{i}\delta}{\mathbf{1} + \mathrm{i}\delta\boldsymbol{\mathcal{E}}_R}\boldsymbol{V}_{RC}, \quad (34)$$

with $\boldsymbol{\mathcal{E}}_{CC}^{(m)} = \frac{1}{2}[\boldsymbol{\mathcal{E}}_{CC}(t_{m+1}) + \boldsymbol{\mathcal{E}}_{CC}(t_m)]$. The source term $S^{(m)}$ describes the injection of density into the region C. For a wave packet initially localized in C the projection onto the left and right electrode $\psi_\alpha^{(0)}$ vanishes and $S^{(m)} = 0$ for any m. The memory term $M^{(m)}$ is responsible for the hopping in and out of the region C. Eq. (33) is the central result of our algorithm for solving the time-dependent Schrödinger equation in extended systems. We refer to Ref. [14] for the implementation details.

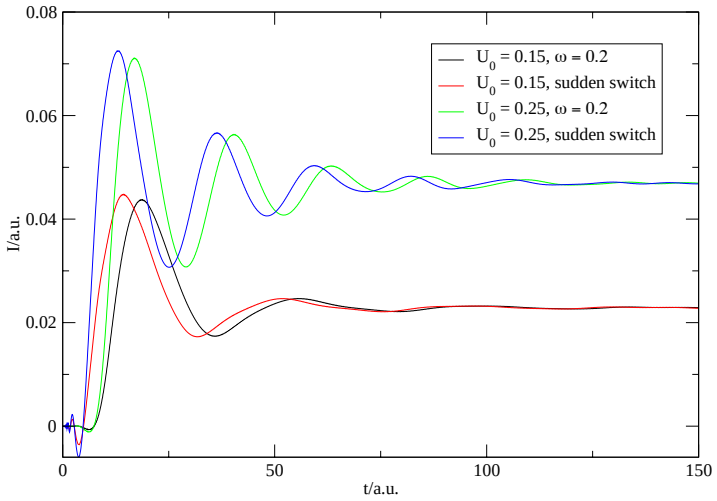

Fig. 3. Time evolution of the current for a double square potential barrier when the bias is switched on in two different manners: in one case, the bias $U_L = U_0$ is suddenly switched on at $t = 0$ while in the other case the same bias is achieved with a smooth switching $U_L(t) = U_0 \sin^2(\omega t)$ for $0 < t < \pi/(2\omega)$. The parameters for the double barrier and the other numerical parameters are described in the main text.

As an example we consider a one-dimensional system of non-interacting electrons at zero temperature where the electrostatic potential vanishes both in the left and right leads. The electrostatic potential in the central region is modeled by a double square potential barrier. Initially, all single particle levels are occupied up to the Fermi energy ε_F. At $t = 0$ a bias is switched on in the leads and the time-evolution of the system is calculated. The numerical parameters are as follows: the Fermi energy is $\varepsilon_F = 0.3$ a.u., the bias is $U_L = 0.15, 0.25$ a.u. and $U_R = 0$, the central region extends from $x = -6$ to $x = +6$ a.u. with equidistant grid points with spacing $\Delta x = 0.03$ a.u.. The electrostatic potential $v_s(x) = 0.5$ a.u. for $5 \leq |x| \leq 6$ and zero otherwise. For the second derivative of the wavefunction (kinetic term) we have used a simple three-point discretization. The energy integral in Eq. (5) is discretized

with 100 points which amounts to a propagation of 200 states. The time step for the propagation was $\Delta t = 10^{-2}$ a.u..

In Fig. 3 we have plotted the total current at $x = 0$ as a function of time for two different ways of applying the bias in the left lead: in one case the constant bias $U_L = U_0$ is switched on suddenly at $t = 0$, in the other case the constant U_0 is achieved with a smooth switching $U_L(t) = U_0 \sin^2(\omega t)$ for $0 < t < \pi/(2\omega)$. As a first feature we notice that a steady state is achieved and that the steady-state current does not depend on the history of the applied bias, in agreement with the results obtained in Section 4. Second, we notice that the onset of the current is delayed in relation to the switching time $t = 0$. This is easily explained by the fact that the perturbation at $t = 0$ happens in the leads only, *e.g.*, for $|x| > 6$ a.u., while we plot the current at $x = 0$. In other words, we see the delay time needed for the perturbation to propagate from the leads to the center of our device region. We also note that the higher the bias the more the current exceeds its steady-state value for small times after switching on the bias.

6 Conclusions

In conclusion, we have described a formally exact, thermodynamically consistent scheme based on TDDFT and NEG in order to treat the time-dependent current response of electrode-junction-electrode systems. Among the advantages we stress the possibility of including the electron-electron interaction not only in the central region but also in the electrodes. We have shown that the steady state develops due to a *dephasing mechanism* without any reference to many-body damping and interactions. The damping mechanism (due to the electron-electron scatterings) of the real problem is described by $v_{\rm xc}$. The nonlinear steady-state current can be expressed in a Landauer-like formula in terms of fictitious transmission coefficients and one-particle energy eigenvalues. Our scheme is equally applicable to time-dependent responses and also allows for calculating the (transient) current shortly after switching on a driving external field. Clearly, its usefulness depends on the quality of the approximate TDDFT functionals being used. Time-dependent linear response theory for dc-steady state has been implemented in Ref. [26] within TDLDA assuming jellium-like electrodes (mimicked by complex absorbing/emitting potentials). It has been shown that the dc-conductance changes considerably from the standard Landauer value. Therefore, a systematic study of the TDDFT functionals themselves is needed. A step beyond standard adiabatic-approximations and exchange-only potentials is to resort to many-body schemes like those used for the characterization of optical properties of semiconductors and insulators [27] or like those based on variational functionals [28]. Another path is to explore in depth the fact that the true exchange-correlation potential is current dependent [29].

We also have shown that the steady-state current depends on the history only through the asymptotic shape of the effective TDDFT potential v_s provided the bias-induced change δv_α is uniform deep inside the electrodes. (This is the anticipated behavior for macroscopic electrodes.) The present formulation can be easily extended to account for interaction with lattice vibrations at a semiclassical level. The inclusion of phonons might give rise to hysteresis loops due to different transient electronic/geometrical device configurations (*e.g.*, isomerisation or structural modification). This effect will be more dramatic in the case of ac-driving fields of high frequencies where the system might not have enough time to respond to the perturbation.

Acknowledgments

This work was supported by the European Community 6th framework Network of Excellence NANOQUANTA (NMP4-CT-2004-500198) and by the Research and Training Network EXCITING. AR acknowledges support from the EC project M-DNA (IST-2001-38051), Spanish MCyT and the University of the Basque Country. We have benefited from enlightening discussions with L. Wirtz, A. Castro, H. Appel, M. A. L. Marques and C. Verdozzi.

References

1. M. Cini, Phys. Rev. B **22**, 5887 (1980).
2. N. D. Lang, Phys. Rev B **52**, 5335 (1995).
3. G. Stefanucci and C.-O. Almbladh, Europhys. Lett. **67**, 14 (2004).
4. P.A. Derosa and J.M. Seminario, J. Phys. Chem. B **105**, 471 (2001).
5. M. Brandbyge, J.-L. Mozos, P. Ordejón, J. Taylor, and K. Stokbro, Phys. Rev. B **65**, 165401 (2002).
6. Y. Xue, S. Datta, and M.A. Ratner, Chem. Phys. **281**, 151 (2002).
7. A. Calzolari, N. Marzari, I. Souza and M. Buongiorno Nardelli, Phys. Rev. B **69**, 035108 (2004).
8. M. D. Ventra, S.T. Pantelides, and N.D. Lang, Phys. Rev. Lett. **84**, 979 (2000).
9. P. S. Krstić, D. J Dean, X. G. Zhang, D. Keffer, Y. S. Leng, P.T. Cummings, J. C. Wells, Comp. Mat. Sci. **28**, 321 (2003).
10. E. Runge and E.K.U. Gross, Phys. Rev. Lett. **52**, 997 (1984).
11. M. Petersilka, U. Gossmann, and E.K.U. Gross, Phys. Rev. Lett. **76**, 1212 (1996).
12. G. Stefanucci and C.-O. Almbladh, Phys. Rev. B **69**, 195318 (2004).
13. F. Evers, F. Weigend, and M. Koentopp, Phys. Rev. B **69**, 235411 (2004).
14. S. Kurth, G. Stefanucci, C.-O. Almbladh, A. Rubio, and E. K. U. Gross, submitted for publication, cond-mat/0502391.
15. M. Di Ventra and T. N. Todorov, J. Phys. C **16**, 8025 (2004).
16. A. Kamenev and W. Kohn, Phys. Rev. B **63**, 155304 (2001).
17. R. van Leeuwen, Phys. Rev. Lett. **80**, 1280 (1998).
18. P. Hohenberg and W. Kohn, Phys. Rev. **136**, B864 (1964).
19. N. D. Mermin, Phys. Rev. **137**, A1441 (1965).

20. A. Blandin, A. Nourtier, and D. W. Hone, J. Phys. (Paris) **37**, 369 (1976).
21. N. S. Wingreen, A-P. Jauho and Y. Meir, Phys. Rev. B **48**, 8487 (1993).
22. A-P. Jauho, N. S. Wingreen and Y. Meir, Phys. Rev. B **50**, 5528 (1994).
23. In principle, there may be degeneracies which require a diagonalisation to be performed for states on the energy shell.
24. Y. Imry, Introduction to Mesoscopic Physics (Oxford University Press, Oxford, 2002).
25. C. Moyer, Am. J. Phys. **72**, 351 (2004); and references therein.
26. R. Baer, T. Seideman, S. Ilani and D. Neuhauser, J. Chem. Phys. **120**, 3387 (2004).
27. A. Marini, R. Del Sole and A. Rubio, Phys. Rev. Lett. **91**, 256402 (2003); L. Reining, V. Olevano, A. Rubio and G. Onida, Phys. Rev. Lett. **88**, 066404 (2002); I. V. Tokatly and O. Pankratov, Phys. Rev. Lett. **86**, 2078 (2001).
28. U. von Barth, R. van Leeuwen, N. E. Dahlen and G. Stefanucci, unpublished.
29. C. A. Ullrich and G. Vignale, Phys. Rev. B **65**, 245102 (2002); and references therein.